Ceramics International 44 (2018) 3649–3657

Contents lists available at ScienceDirect

Ceramics International

journal homepage: www.elsevier.com/locate/ceramint

Phase formation and crystallization kinetics in cordierite ceramics prepared from kaolinite and magnesia

Djaida Redaoui[a,b], Foudil Sahnoune[b,c], Menad Heraiz[a,b], Nouari Saheb[d,*]

[a] Physics and Chemistry of Materials Lab, Department of Physics, University Mohamed Boudiaf of M'sila, 28000 M'sila, Algeria
[b] Department of Physics, Faculty of Science, University Mohamed Boudiaf of M'sila, 28000 M'sila, Algeria
[c] Research Unit on Emerging Materials (RUEM), Ferhat Abbas of Setif 01, Setif 19000, Algeria
[d] Department of Mechanical Engineering, King Fahd University of Petroleum and Minerals, Dhahran 31261, Saudi Arabia

ARTICLE INFO

Keywords:
A. Solid state reaction
D. Clays
D. Cordierite
D. MgO

ABSTRACT

In this work, Algerian kaolinite, a naturally occurring clay mineral, was used as low-cost precursor for the synthesis of cordierite ceramics. The kaolinite was mixed with synthetic magnesia, and the mixture was ball milled and reaction sintered in the temperature range 900–1350 °C for 2 h. Thermogravimetry (TG), differential thermal analysis (DTA), dilatometry, high temperature x-ray powder diffraction (XRD), Raman spectroscopy, and scanning electron microscopy (SEM) complementary techniques were used to analyze sintering behavior, characterize phase transformations, and investigate crystallization kinetics. Milling the kaolinite and magnesia mixture for 10 h yielded a homogenous powder, decreased the average particle size, and improved the roundness of particles. Different crystalline phases were present in the samples sintered in the temperature range 900–1150 °C, the cordierite phase started to crystallize at 1200 °C, and the formation of highly dense cordierite (99%) was complete at 1250 °C. The activation energy values for cordierite formation calculated using Kissinger, Boswell, and Ozawa methods were found to be equal to 577, 589, and 573 kJ/mol, respectively. The kinetic parameters n and m had values close to 2. Bulk nucleation with a constant number of nuclei was the dominant mechanism in cordierite crystallization, followed by two-dimensional growth controlled by interface reaction.

1. Introduction

Cordierite, an aluminum magnesium silicate material, is one of the most attractive advanced ceramic materials for functional applications because of its very low thermal expansion, low electrical conductivity, high chemical stability, high corrosion resistance, and good mechanical strength [1,2]. Ceramic materials based on cordierite find applications as packaging materials, refractory components, turbine heat exchanger components, products with high thermal shock resistance, and supports for catalysts in diesel cars [1–5]. Furthermore, cordierite based materials are potential candidates in geo-barometry and geo-thermometry [6], and thermal insulation [7] applications.

Because of the low quality and scarcity of natural cordierite in earth [8], researchers have used various starting raw materials and different processing methods to synthesize cordierite and cordierite based ceramics. Cordierite, with $2MgO.2Al_2O_3.5SiO_2$ chemical composition and $Mg_2Al_4Si_5O_{18}$ chemical formula, is considered the most important phase in the MgO-Al_2O_3-SiO_2 phase diagram. Stoichiometric cordierite is usually synthesized at temperatures higher than 1430 °C [9]. Nevertheless, cordierite ceramics with high volume fraction of the cordierite phase could be prepared, from costly precursors, at relatively lower temperatures using many methods including co-precipitation [9–11], the Pechini method [12], sol-gel [13–15] or recrystallization of molten glasses [16,17]. Additionally, high melting temperatures as high as 1600 °C are required in the case of glass ceramics. Therefore, due to their low cost, natural raw materials [7,18–22] and solid-state synthesis method [1,7,18–23] remained the most attractive precursors and process, respectively, for the preparation of cordierite based materials. In solid-state synthesis, chemical reaction between the starting minerals and/or raw materials as well as densification could be attained in a one-step simple heat treatment [24].

The kinetics of cordierite formation was investigated by many researchers [25–36]. Donald [30] analyzed cordierite formation using DTA and DSC under both isothermal and non-isothermal conditions and reported values of 532–574 kJ/mol for the glass to μ-cordierite transformation and 399–426 kJ/mol for the μ-cordierite to α-cordierite transformation. Kim and Lee [31] used non-isothermal DTA to investigate cordierite formation from stoichiometric and CeO_2 doped starting glass systems. They reported average activation energies of 653 kJ/mol for a stoichiometric starting glass and 418 kJ/mol for a

* Corresponding author.
E-mail address: nouari@kfupm.edu.sa (N. Saheb).

https://doi.org/10.1016/j.ceramint.2017.11.119
Received 28 October 2017; Received in revised form 16 November 2017; Accepted 17 November 2017
Available online 21 November 2017

CeO_2 doped starting glass. Song el al. [34] investigated cordierite formation, in cordierite glass-ceramics fabricated from potassium feldspar, using non-isothermal DSC. They reported activation energies of 230.77–279.81 kJ/mol and 348.85–374.33 kJ/mol for the one fold α-cordierite and the concurrent precipitation of α-cordierite and leucite, respectively. Goel and co-workers [35] studied cordierite formation, in MgO-Al_2O_3-SiO_2-TiO_2 glass system, under non-isothermal conditions using DTA. They obtained activation energy values of 340 and 498 kJ/mol for the crystallization of μ-cordierite and α-cordierite, respectively. Hu and Tsai [36] investigated the formation of the cordierite-type ($MgAl_{1.83}S_{2.25}O_y$) glass with and without BaO addition by non-isothermal DTA. They reported activation energy of 366 kJ/mol in BaO free samples and 290–487 kJ/mol in BaO added samples. Silva et al. [29] used DTA to investigate the kinetics of cordierite crystallization, under non-isothermal conditions, from diphasic gels obtained from colloidal silica, magnesium and aluminum nitrates, and citric acid. The apparent activation energy value for cordierite crystallization was 467 kJ/mol. Goel et al. [32] used non-isothermal DTA to study the formation of cordierite in NiO-doped glasses. They got values of 300 kJ/mol for the glass to μ-cordierite crystallization and 500 kJ/mol for the μ-cordierite to α-cordierite transformation for a NiO-doped system.

Watanabe and Giess [27] investigated crystallization kinetics of cordierite formation from a glass in the presence P_2O_5 and B_2O_3 additives, under isothermal conditions, using DTA and XRD. They reported values of 303.5 and 301.9 kJ/mol for activation energy calculated from DTA and x-ray diffraction data. Rudolph et al. [28] utilized an isothermal static experiment and a dynamic non-isothermal DTA to characterize cordierite formation from a glass modified with P_2O_5. The authors reported a value of 469 kJ/mol for the activation energy obtained from the static experiment, and values of 300 and 470–500 kJ/mol for the activation energy calculated using the peak maximum temperature and the peak start temperature in DTA experiment, respectively. They found that the activation energies obtained using the peak start temperature in DTA dynamic experiment were very close to those obtained from the static experiment. Boudchicha et al. [33] analyzed cordierite formation, in glass ceramics prepared from kaolin and dolomite, using non-isothermal x-ray analysis and reported an activation energy value of 450 kJ/mol. Miller and Misture [25] used isothermal time-resolved powder diffraction and non-isothermal DTA to investigate the kinetics of cordierite formation. They obtained activation energies of about 600 kJ/mol for the glass to μ-cordierite transformation and between 800 and 850 kJ/mol for the μ-cordierite to α-cordierite transformation. Clark [26] developed equations based on the nucleation and growth principle for two sequential reactions and used them to analyze cordierite formation from a glass precursor with and without doping with zinc. He used data obtained from isothermal, time resolved, powder diffraction method to determine the kinetics of the two-step consecutive reaction. He obtained activation energies (isothermal) of 271 and 221 kJ/mol for glass to μ-cordierite transformation without doping with zinc; and 179 and 170 kJ/mol for the μ-cordierite to α-cordierite transformation without doping with zinc.

Analysis of the literature [25–36] shows significant variation in the activation energy values reported for the formation of cordierite. The discrepancies were believed to be due to the methods of sample preparation, data collection, or data analysis [26]. Furthermore, the type and composition of natural raw materials, additives, and the presence of trace elements [17,25,26] were found to have direct influence on the rate of cordierite formation and the properties of the final product. In previous works, the authors used Algerian kaolinite to synthesize mullite through reaction sintering it with high purity alumina [37] and utilized DTA to study the kinetics of its dehydroxylation [38] and formation [39]. The objective of the present work is to explore the possibility to synthesize low-cost cordierite ceramic materials from Algerian kaolinite, a natural low-cost and abundant raw material, and synthetic magnesia. Two types of raw kaolinite from east Algeria was used, the first kaolinite rich of Al_2O_3 and the second rich of SiO_2. Stoichiometric mixture of the kaolinite and magnesia was ball milled, to promote the formation of cordierite and densification [20], and then reaction sintered to produce dense cordierite ceramics. Complementary techniques were used to: (i) characterize the formation of phases and their transformations, (ii) analyze sintering behavior, and (iii) investigate the crystallization kinetics. The Kissinger, Boswell, and Ozawa methods were used to calculate the values of the activation energy and kinetic parameters, for cordierite formation under non-isothermal conditions.

2. Materials and methods

2.1. Raw materials and processing

Kaolinite (DD1 sample) collected from Djebel Debagh (Guelma, East Algeria) and Tamazarte kaolinite (TK sample) collected from Jijel, East Algeria, were used in this investigation. The DD1 and TK kaolinite samples were used as sources of Al_2O_3 and SiO_2, respectively. A mixture of DD1, TK, and synthetic magnesia powders (DTM) at weigh ratios of 59, 29, 12%, respectively, was prepared to obtain stoichiometric cordierite which theoretically contains 13.8% of MgO, 34.9% of Al_2O_3 and 51.4% of SiO_2 [1]. Sixteen grams of the kaolinite and MgO mixture, 15 zirconia balls (diameter of 10 mm), and 120 ml of ethanol were loaded into zirconia vials of 250 ml in volume. A Fritsch P6 ball mill was used to perform the mixing and milling experiments for different times at room temperature using a speed of 250 rev/min. The obtained slurry was dried in a furnace at 150 °C for 24 h, and then cold pressed at 75 MPa to produce cylindrical specimens (13 mm diameter). The compacted powders were sintered in the temperature range 900–1350 °C for 2 h.

2.2. Characterization methods

A LABSYS EVO DTA/DSC-TG SETARAM equipment was used to perform the TG and DTA experiments. The samples were heated to 1400 °C under argon gas flowing at a rate of 40 cm^3/min. Heating rates of 10, 20, 30, 40, and 50 °C/min were used. Dilatometry experiments were carried out up to 1320 °C at a heating rate of 5 °C/min using NETZSCH (Dil 402 C) equipment. A reference sample made of α-Alumina having the same dimensions was used. A diffractometer system (XPERT-Pro) with Cu-K_α radiation of a wavelength 0.15418 nm was used to characterize the raw powders as well as sintered samples. A KERN densimeter was used to determine the bulk density of samples following the water immersion method. The raw powders and consolidated samples were analyzed using JEOL SEM model JSM-7001F. Raman spectroscopy measurements were carried out using BRUKER SENTERRA equipment.

2.3. Calculation methods

The non-isothermal activation energy (E_A) for cordierite formation was calculated using Kissinger [40,41], Boswell [42], and Ozawa [43] methods according to Eqs. 1–3, respectively, as expressed bellow:

$$\ln\left(\frac{\varphi}{T_p^2}\right) = -\frac{E_A}{RT_p} + C_1 \quad (1)$$

$$\ln\left(\frac{\varphi}{T_p}\right) = -\frac{E_A}{RT_p} + C_2 \quad (2)$$

$$\ln(\varphi) = -1.0518\frac{E_A}{RT_p} + C_3 \quad (3)$$

Where φ[°C/min], E_A [kJ/mol], T_p[°C] and R, are the heating rate, activation energy, absolute peak temperature in DTA curves, and the

Table 1
Chemical composition of kaolinite (wt%).

Kaolinite	Al_2O_3	SiO_2	Na_2O	SO_3	K_2O	MgO	CaO	MnO	Fe_2O_3	TiO_2	LOI
TK	19.29	69.86	0.13	0.03	2.67	0.4	0.4	–	0.72	0.4	6.31
DD1	39.13	45.30	0.04	–	0.21	0.05	0.15	0.02	0.07	–	14

universal gas constant, respectively.

The value of the Avrami parameter n, which indicates the crystallization mode, was calculated using the following equation [44–46]:

$$n = \frac{2,\ 5T_p^2 R}{\Delta T_p E_A} \quad (4)$$

Where ΔT_p is the full width, at the half-maximum intensity, of the exothermic peak.

The value of the kinetic parameter m, which indicates the dimensionality of crystal growth, was calculated using the Matusita equation (Kissinger modified equation) [45]:

$$\ln\left(\frac{\varphi^n}{T_p^2}\right) = C_3 - \frac{mE_A}{RT_p} \quad (5)$$

3. Results and discussion

3.1. Processing of powders

The chemical composition of DD1 and TK raw kaolinite is presented in Table 1. The SiO_2 content SiO in DD1 kaolinite is 45.3 wt% compared with 62.1 wt% in Malaysian kaolinite [47], 53.7 wt% in French kaolinite [48], and 52.8 wt% in American kaolinite [49]. The Al_2O_3 content is 39.13 wt% compared with Malaysian kaolinite 36.8 wt% [47], French kaolinite 41.8 wt% [48], and American kaolinite 44.7 wt% [49]. The SiO_2 and Al_2O_3 contents in TK kaolinite are 69.86 and 19.29 wt%, respectively. The TK kaolinite is very rich of SiO_2 but it has low content of Al_2O_3. The chemical composition of DD1 and TK kaolinite shows that they are suitable sources of Al_2O_3 and SiO_2, respectively. The influence of mechanical milling on the particle size of the DTM powder is shown in Fig. 1(a). The cumulative distribution was used to obtain the average particle size as a function of milling time as presented in Fig. 1(b). It can be noticed that the average particle size decreased rapidly with the increase in milling time up to 10 h, then did not change significantly with further increase in milling time. Fig. 2 shows SEM images of unmilled kaolinite and the DTM powder milled for 10 h. The particles of unmilled raw kaolinite powder have large size and irregular shapes. However, milling the DTM powder for 10 h yielded a homogenous powder with particles having small size and more rounded shape. It was reported that milling of precursors promotes the formation of large amount of cordierite and improves the densification of sintered samples [20].

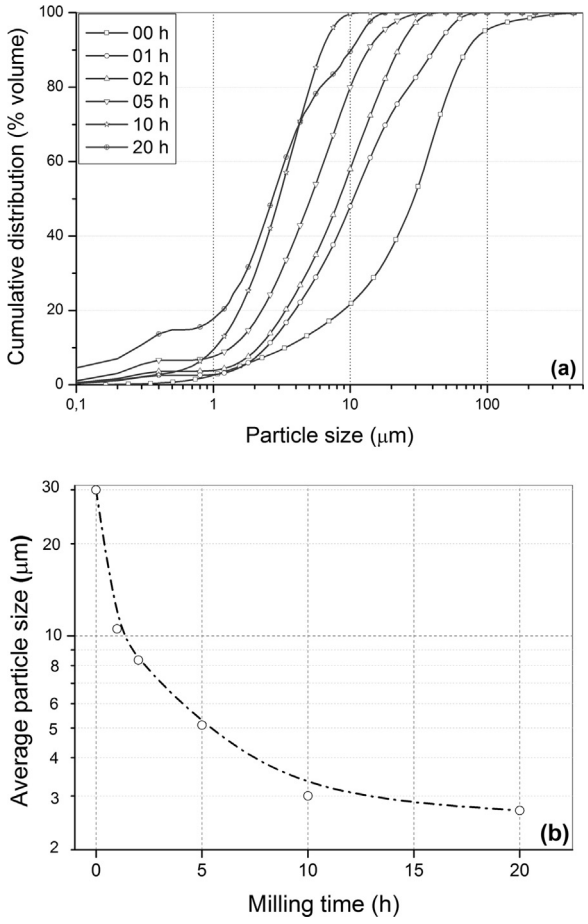

Fig. 1. Effect of milling time on particle size distribution (a) and average particle size (b) of kaolinite and MgO powder mixture.

3.2. Phase transformations

TG/DTA, DTG curves of DTM powder mixture heated from room temperature to 1400 °C (heating rate of 30 °C/min) are presented in Fig. 3. Two endothermic peaks at 140 and 560 °C, and two exothermic peaks at 977 and 1184 °C are present. The first mass loss (about 1.5 wt %) in the temperature range 50–230 °C is due to the evaporation of adsorbed water and corresponds to the first DTA peak at 140 °C. The second mass loss (about 12.5 wt%) in the temperature range 400–560 °C is due to the dehydroxylation of the kaolinite and the formation of metakaolinite, which correlates with the second DTA peak at 560 °C. The mass loss remained constant above 680 °C. The first exothermic DTA peak at 998 °C correspond to the formation of mullite. This is in agreement with the findings of Almeida at al. [1] who reported a temperature between 900 and 1000 °C for the nucleation of mullite, depending on the composition of the raw material used. The second exothermic DTA peak at 1153 °C correspond to the formation of α- cordierite phase.

Fig. 4 shows the influence of heating rate on DTA curves of DTM mixture. Endothermic peaks between 50 and 700 °C and exothermic peaks between 950 and 1250 °C are present. The weak endothermic peaks centered at 130 °C are due to the evaporation of adsorbed water. The strong endothermic peaks centered at 560 °C are due to the dehydroxylation of kaolinite and the formation of metakaolinite. The exothermic peaks in the temperature ranges 950–1050 °C and 1120–1250 °C are due to the formation of mullite and α- cordierite phases, respectively. The curves shows clearly that increasing heating rate from 10 to 50 °C/min shifted the maximum of the peak position to higher temperature.

The influence of temperature on cordierite crystallization and the weight fraction of crystalline phases, present in samples sintered at different temperatures for 2 h, are shown in Figs. 5 and 6, respectively. The phases present in the sample sintered at 950ºC were sapphirine ($Mg_{19.12}Al_{45.24}Si_{11.64}O_{80}$), quartz ($SiO_2$) and magnesium silicate (Mg_2SiO_4) and their weight fractions were 66, 12, and 22 wt%, respectively. The magnesium silicate phase disappeared, the fractions of

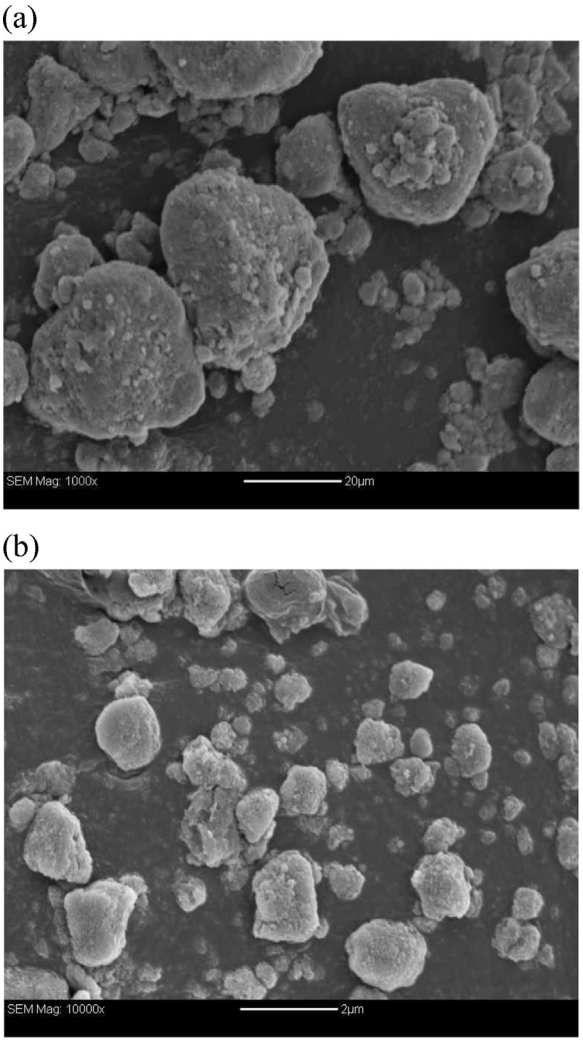

Fig. 2. SEM images of kaolinite powder before milling (a) and kaolinite and MgO powder mixture milled for 10 h (b).

sapphirine and quartz decreased to 48 and 7 wt%, respectively, and mullite ($Al_{4.5}Si_{1.5}O_{9.74}$) started to form in the sample consolidated at 1000 °C. The fraction of mullite phase increased to 48 wt% with the increase in temperature to 1100 °C, then decreased to 11 wt% at 1150 °C. The reflections of the mullite phase disappeared in the

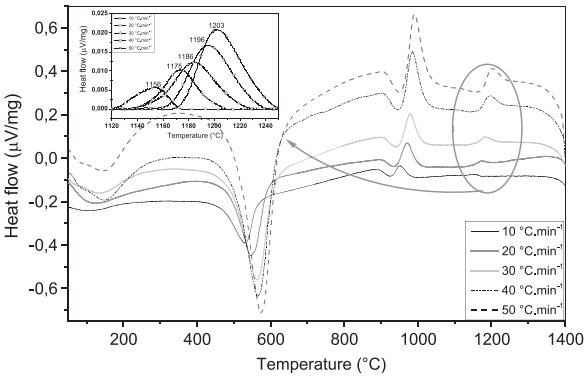

Fig. 4. DTA curves of kaolinite-magnesia mixture (at different heating rates).

spectrum of the sample sintered at 1200 °C. The cristobalite phase (SiO_2) was present in small fractions of 9 and 6 wt% in samples consolidated at 1150 and 1200ºC, respectively. The µ-cordierite phase ($Mg_8Al_{16}Si_{20}O_{72}$) started to crystallize at 1200 °C, and at 1250 °C the α-cordierite crystallization process begins simultaneously with µ-cordierite ($Mg_4Al_8Si_{10}O_{36}$) crystallization. At 1300 and 1350 °C, the fraction of α-cordierite increased to 85 and 96 wt%, respectively, while the fraction of µ-cordierite decreased to 15 and 4 wt%. Cordierite was reported to form at 1250 °C [1], or between 1100 and 1250 °C [23].

Fig. 7 shows shrinkage curves for DTM mixture heated to 1320 °C at 5 °C/min. It can be clearly seen that transformations occurred in six stages labeled A, B, C, D, E, and F. Stage A is characterized with a relative linear expansion between 25 and 160 °C due to the evaporation of adsorbed water, this is in agreement with the TG/DTA results discussed earlier. Stage B started at 510 °C and ended at 605 °C, and is characterized with a small relative linear shrinkage (about 2%) and a maximum rate of shrinkage at 568 °C. The shrinkage results from the dehydroxylation of kaolinite and the formation of metakaolinite, and corresponds to the endothermic peak at 565.4 °C seen in the DTA curve presented in Fig. 4. Stage C, which starts at 718 °C and extends to 975 °C, as can be seen in Fig. 7(b), is characterized with a large relative linear shrinkage (about 21.5%). This large shrinkage is due to two transformations. The first denoted C_1 and corresponds to the formation of Al–Si spinel phase, with a maximum rate at 884 °C; and the second denoted C_2 and corresponds to the formation of magnesium silicate and quartz with a maximum rate at 918 °C. Stage D starts at 975 °C and extends to 1150 °C, as can be seen in Fig. 7(c), and is characterized with a small relative linear shrinkage (about 3%). This small shrinkage is due to two transformations. The first denoted D_1 and corresponds to the formation of mullite and cristobalite phases which increases with the

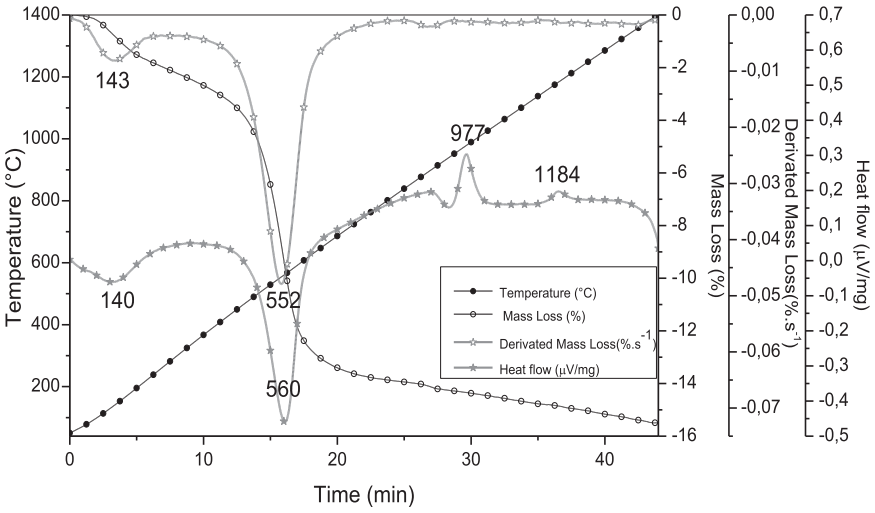

Fig. 3. DTA/TG, DTG curves of kaolinite-magnesia mixture (heating rate 30 °C/min).

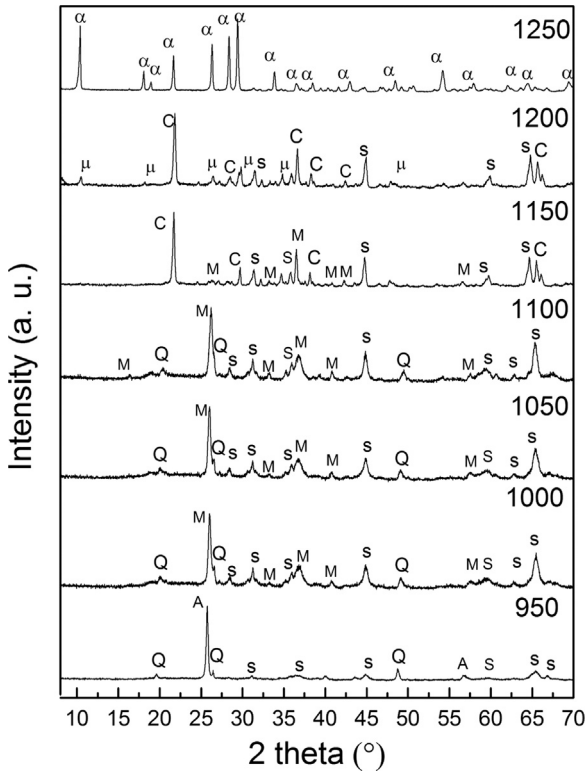

Fig. 5. XRD patterns of DTM powder treated at different temperatures for 2 h. A: magnesium silicate, Q: quartz, M: mullite, S: sapphirine, C: cristobalite, μ: μ- cordierite and α: α- cordierite.

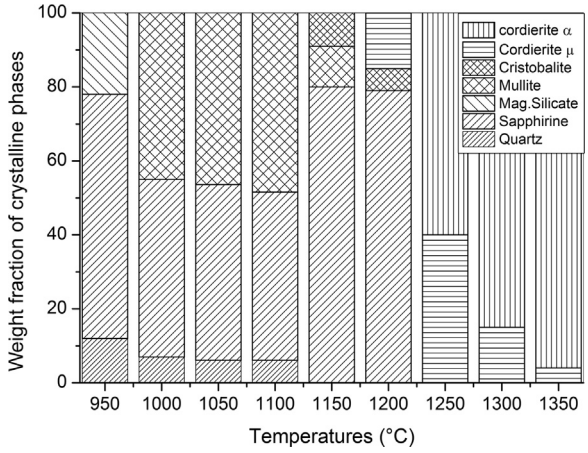

Fig. 6. Weight fraction of crystalline phases present in samples sintered at different temperatures for 2 h.

increase in heating temperature from 1075 to 1150 °C. The second denoted D_2 and corresponds to the formation of sapphirine with a maximum speed at 1071.5 °C. The expansion seen in stage E, between 1235 and 1350 °C, is due to the formation of cordierite, while, the expansion seen in stage F, between 1340 and 1358 °C, might be due to the presence of a glass phase.

Raman spectra of samples sintered at different temperatures for 2 h are presented in Fig. 8. For the sample sintered at 950 °C, the high intensity peaks at 393, 461, 507, 580, and 634 cm^{-1}, and the low intensity peaks at 822 and 858 cm^{-1} are characteristic peaks of the sapphirine and magnesium silicate phases, respectively. In addition to these peaks, a peak at 406 cm^{-1} characteristic of mullite appeared in the spectrum of the sample sintered at 1000 °C. Peaks of magnesium silicate disappeared from the spectrum of the sample sintered at 1050 °C, and only mullite peaks (at 406 and 560 cm^{-1}) and sapphirine peaks (at 461, 507, 580, and 634 cm^{-1}) were present. The new peaks which appeared at 253, 445, and 611 cm^{-1} in Raman spectrum of the sample sintered at 1100 °C were attributed to mullite. For the sample sintered at 1150 °C, peaks at 253 and 507 cm^{-1}, characteristic of mullite and sapphirine, respectively, are still present, the other peaks at 253, 370, 507, 565, 670, 975, 1014 cm^{-1}, were attributed to cordierite. Raman peaks at 256, 292, 370, 435, 487, 565, 670, 975, 1014, and 1190 cm^{-1} present in spectra of samples sintered at 1200, 1250, 1300, and 1350 °C were attributed to the cordierite phase. Peaks characteristic of mullite and sapphirine phases disappeared from the spectra indicating that cordierite formation was complete [50].

3.3. Kinetic parameters

Plots of Y versus $(1/T_p)$, obtained using Kissinger, Boswell, and Ozawa methods, for α- cordierite formation at various heating rates are shown in Fig. 9. The values of the activation energy of cordierite formation calculated from the slope of the function $Y = f(1/T_p)$ and the values of coefficient of determination R^2 are listed in Table 2. The activation energy values for the formation of the cordierite phase, calculated from non-isothermal DTA results using Kissinger, Boswell and Ozawa methods, were 577, 589 and 573 kJ/mol, respectively. These values are comparable with those of 532–574 kJ/mol reported by Donald [30], for the glass to μ-cordierite transformation. The average activation energy value of 580 kJ /mol obtained in this work, is comparable with that of about 600 kJ/mol obtained for the glass to μ-cordierite transformation, and is lower than that of 800 and 850 kJ/mol reported for the μ-cordierite to α-cordierite transformation [25]. Also, it is lower than the average activation energy of 653 kJ/mol obtained for the formation of cordierite from a stoichiometric starting glass as reported by Kim and Lee [31]. However, it is larger than the activation energy values between 170 and 500 kJ /mol reported by other researchers [25–36]. The discrepancy in the reported activation energy values might be attributed to the different methods of sample preparation, data collection, or data analysis [26]. It is worth mentioning here that the kinetics of cordierite formation was investigated under isothermal [25–27,30] and non-isothermal [25,28–36] conditions, and different techniques including DTA [28–32,35,36], DSC [30,34], x-ray diffraction [27,33], and time resolved powder diffraction [25,26], were used to determine the activation energy values. Additionally, in some studies, additives such as P_2O_5 and B_2O_3 [27], P_2O_5 [28], CeO_2 [31], and NiO [32], BaO [36], and zinc [26] were added to the raw materials which influenced the formation of cordierite.

The values of the Avrami parameter n, which depicts the crystallization mode, for heating rates from 10 to 50 °C/min, were determined using Eq. (4) and presented in Table 3. The average value of the Avrami parameter is 2.12. This value is close to 2, which indicates that cordierite crystallization is controlled by the interface reaction. Plots of $\ln(\varphi^n/T_p^2)$ versus $1/T_p$ obtained using Matusita method (Eq. (5)) are shown in Fig. 10. The dimensionality of crystal growth, m, calculated from the slope of the function, is found to be equal to 2.05 for cordierite formation. Both the growth morphology parameters n and m are close to 2. These results show that the bulk nucleation with constant number of nuclei is the dominant mechanism in cordierite crystallization followed by two-dimensional growth with plates morphology controlled by the interface reaction [45,47].

3.4. Densification and microstructure

The change in the bulk density of samples is shown in Fig. 11. The density increased from 2.11 to 2.51 g/cm^3 with the increase in sintering temperature from 900 to 1200 °C, then decreased to 2.50, 2.46, and 2.42 g/cm^3 with further increase in sintering temperature to 1250, 1300, and 1350 °C, respectively. The increase in the bulk density is due to the decrease in the amount of pores during sintering. Furthermore, it

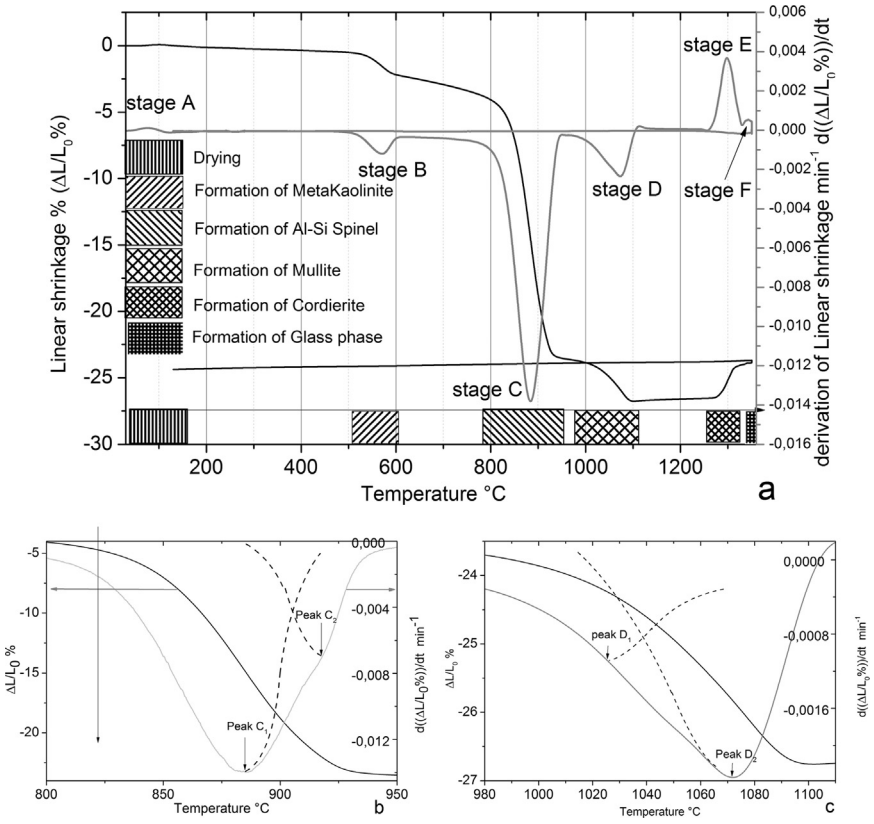

Fig. 7. Dilatometry curves of kaolinite-magnesia mixture. (**a**: shrinkage (expansion) curves and first derivatives of shrinkage (expansion) curves, **b**: Stage C and **c**: stage D).

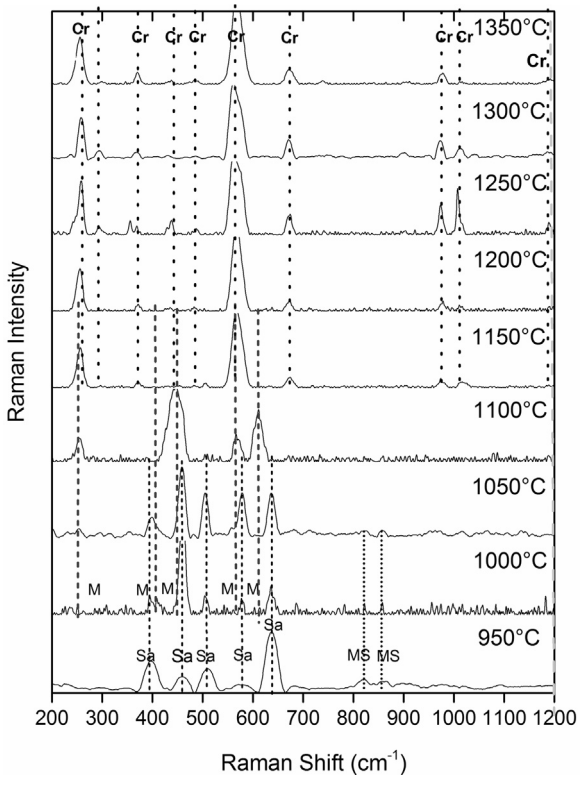

Fig. 8. Raman spectra of DTM powder sintered at different temperatures (MS: aluminum silicate, M: mullite, Sa: sapphirine and Cr: cordierite).

was reported that "densification is usually enhanced in homogeneous powder compacts in which particles are packed to high relative density and large pores and powder agglomerates are absent" [49,51]. It is believed that the small particle size and the rounded shape of the particles of the milled powder had enhanced sintering and improved densification as a result of the small diffusion path and the large surface area associated with the fine particles. The bulk density value of 2.50 g/cm^3 obtained at 1250 °C is very close to 2.53 g/cm^3, the bulk density value of cordierite [1]. This suggests that the formation of highly dense cordierite (relative density of almost 99%) was complete at 1250 °C. The decrease in bulk density with further increase in temperature to 1250 and 1350 °C might be due to the presence of a glassy phase [52]. The dilatometry results recorded between 1340 and 1358 °C showed the possibility of the presence of a glassy phase. It is worth mentioning here that cordierite melts at 1470 °C, and sintering temperatures as high as 1300 and 1350 °C might lead to the formation of a liquid phase which decreases the bulk density. The density value of 2.50 g/cm^3 obtained for the sample sintered at 1250 °C for 2 h is comparable with the values of 2.58 and 2.52 g/cm^3 reported for cordierite samples synthesized from natural zeolite, MgO, and Al_2O_3 mixture mechanically activated for 0.5 and 2 h, respectively, and sintered at 1250 °C for 1 h [52]. The density values of 2.46 and 2.42 g/cm^3 obtained for samples sintered at 1300 and 1350 °C for 2 h, respectively, are in good agreement with the value of 2.4 g/cm^3 reported for cordierite synthesized by solid-state reaction sintering of Moroccan stevensite and andalusite at 1300 °C for 2 h [53]. The density value of 2.46 g/cm^3 achieved for the sample sintered at 1300 °C for 2 h is slightly higher than that of 2.33 g/cm^3 reported for the sample produced from mechanically activated kaolin/talc/boehmite powders and sintered at 1300 °C for 2 h [54]. The density value of 2.42 g/cm^3 achieved for the sample sintered at 1350 °C for 2 h is slightly lower than that of 2.58 g/cm^3 reported for cordierite ceramics obtained for samples produced from mechanically activated kaolin/talc/alumina powders and sintered at 1350 °C for 1 h [55].

Typical SEM images of surfaces of a fractured and polished sample sintered at 1300 °C for 2 h are shown in Fig. 12. The sintered sample has a homogeneous microstructure and uniform distribution of small pores (smaller than 10 μm) and cordierite grains with small average grain size of about 3 μm. The morphology of cordierite crystals is known to

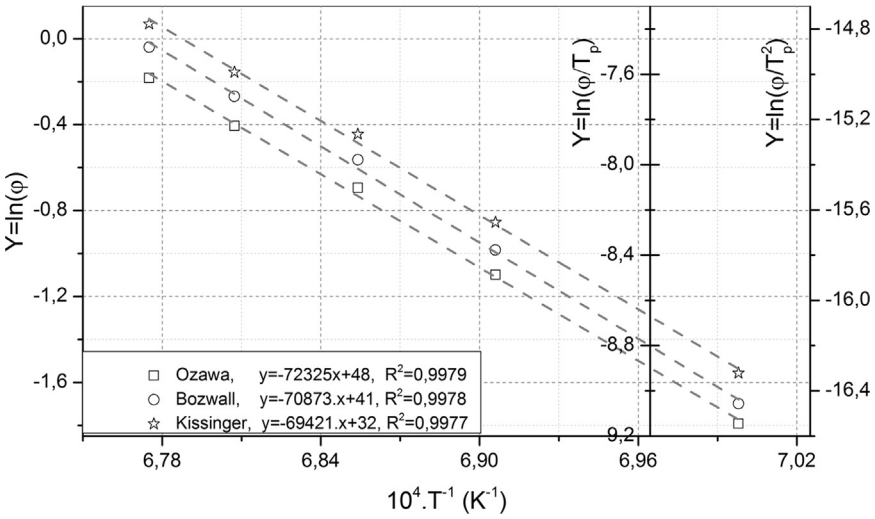

Fig. 9. Plots of Y versus $(1/T_p)$ of α- cordierite formation at various heating rates.

Table 2
Activation energy (E_A) and the coefficient of determination (R^2) of α- cordierite formation calculated using different methods.

Method	Kissinger	Boswell	Ozawa
Activation energy E_A (kJ/mol)	577	589	573
Coefficient of determination (R^2)	0,9977	0,9978	0,9979

Table 3
Avrami parameter n obtained from *DTA* experiments performed at different heating rates.

Heating rates (°C/min)	10	20	30	40	50
ΔT	32	34	37	38	39
T_p peak	1156	1173	1184	1194	1203
Avrami parameter (n)	2.30	2.21	2.06	2.04	2.01

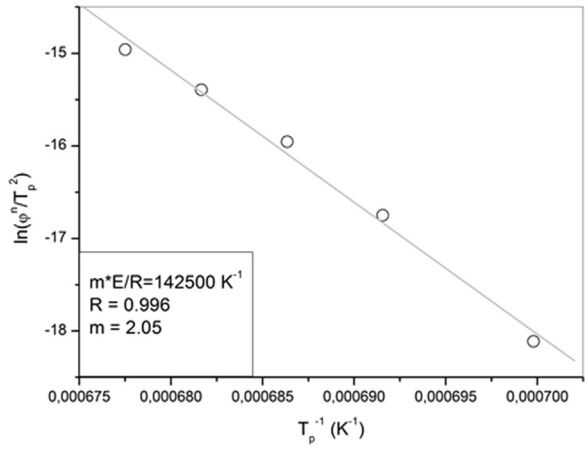

Fig. 10. Plot of $\ln(\varphi^n/T_p^2)$ versus $1/T_p$ according to Matusita equation.

depend on the composition of precursors [1]. The micrographs presented in Fig. 12 support the results obtained from TDA, XRD, Raman spectra and dilatometry experiments, which confirmed the presence of cordierite phase in the DTM mixture sintered at 1300 °C. Similar results were reported by Bejjaoui and co-workers [53] who confirmed the formation of monolithic cordierite, from Moroccan stevensite and andalusite, in samples sintered at 1350 °C for 2 h. Additionally, it supports the findings of Almeida [1] who obtained cordierite from compositions containing kaolin waste, talc, and magnesium oxide and concluded that cordierite nucleation started at 1250 °C and intensified at 1350 °C.

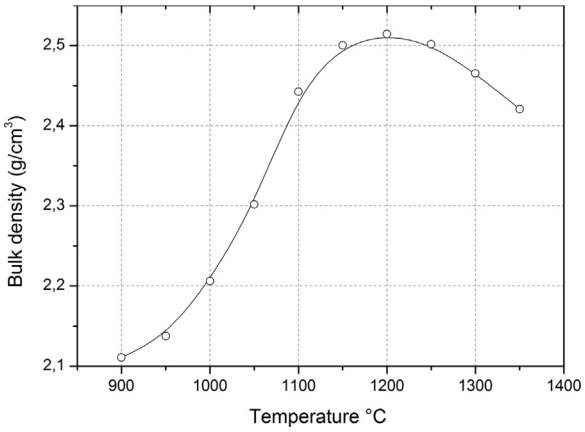

Fig. 11. Bulk density of samples sintered at different temperatures.

The results of this study revealed the possibility to synthesize highly-dense and low-cost cordierite through milling and reaction sintering Algerian kaolinite and magnesia. Cordierite ceramic materials are of great industrial importance because of their low cost [1] and negative thermal expansion along the C direction, which leads to significant improvement in thermal shock resistance and reduction in thermal conductivity [56]. This work focused on the synthesis and crystallization behavior of cordierite. The mechanical and thermal properties of the developed material will be the subject of future work.

4. Conclusion

Low-cost cordierite ceramics were successfully prepared by ball milling and reaction sintering of Algerian kaolinite and synthetic magnesia. Complementary techniques were used to characterize phase transformations, sintering behavior, and crystallization kinetics. Activation energies, for cordierite formation, and growth morphology parameters were evaluated using Kissinger, Boswell, and Ozawa methods. Milling the kaolinite and magnesia mixture for 10 h yielded a homogenous powder, decreased the average particle size, and improved the roundness of particles. Different crystalline phases were present in the samples sintered in the temperature range 900–1150 °C, the cordierite phase started to crystallize at 1200 °C, and the formation of highly dense cordierite (99%) was complete at 1250 °C. The activation energy values for cordierite formation calculated using Kissinger, Boswell, and Ozawa methods were found to be equal to 577, 589, and 573 kJ/mol, respectively. The kinetic parameters n and m had values close to 2. Bulk nucleation with a constant number of nuclei was the

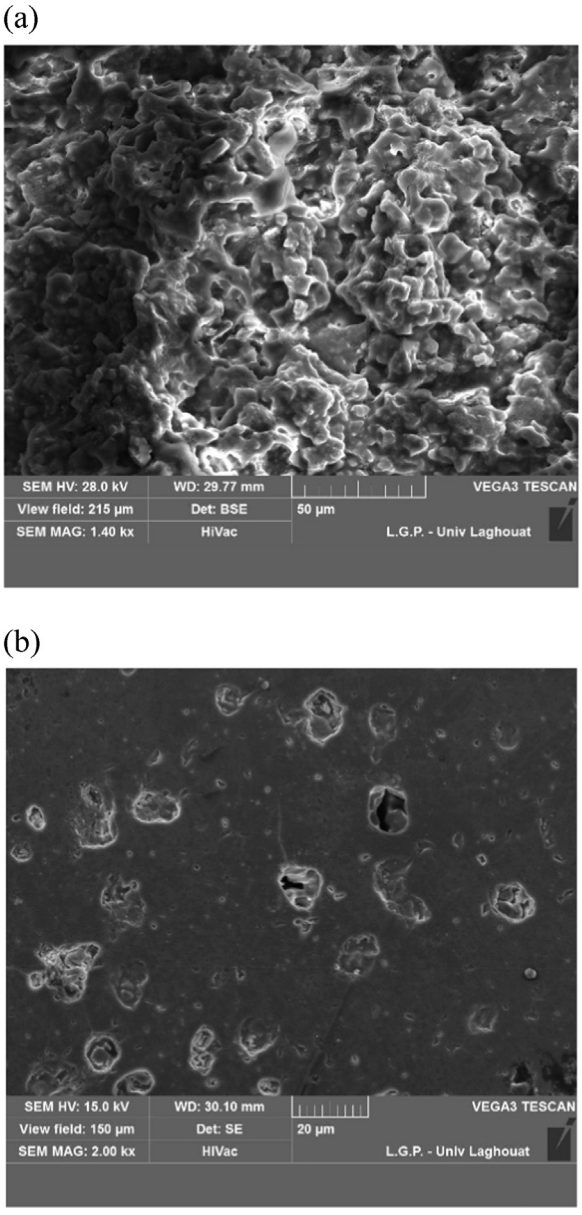

Fig. 12. SEM images of surfaces of (a) fractured and (b) polished samples sintered at 1300 °C for 2 h.

dominant mechanism in cordierite crystallization, followed by two-dimensional growth controlled by interface reaction.

References

[1] EsterPiresde Almeida, IgorPereirade Brito, HeberCarlos Ferreira, HélioLirade Lucena, LisianeNavarrodeLima Santana, Gelmiresde AraújoNeves, Cordierite obtained from compositions containing kaolin waste, talc and magnesium oxide, Ceram. Int. 〈http://dx.doi.org/10.1016/j.ceramint.2017.10.102〉.

[2] D. Njoya, A. Elimbi, D. Fouejio, M. Hajjaji, Effects of two mixtures of kaolin-talc-bauxite and firing temperatures on the characteristics of cordierite- based ceramics, J. Build. Eng. 8 (2016) 99–106.

[3] P. Rohan, K. Neufuss, J. Matejicek, J. Dubsky, L. Prchlik, C. Holzgartner, Thermal an mechanical properties of cordierite, mullite and steatite produced by plasma spraying, Ceram. Int. 30 (2004) 597–603.

[4] N.E. Hipedinger, A.N. Scian, E.F. Aglietti, Magnesia–ammonium phosphate-bonded cordierite refractory castables: phase evolution on heating and mechanical properties, Cem. Concr. Res. 34 (2004) 157–164.

[5] Y. Dong, X. Feng, D. Dong, S. Wang, J. Yang, J. Gao, X. Liu, G. Meng, Elaboration and chemical corrosion resistance of tubular macro-porous cordierite ceramic membrane supports, J. Membr. Sci. 304 (2007) 65–75.

[6] B. Mukhopadhyay, M.J. Holdaway, Cordierite-garnet-sillimanite-quartz equilibrium: I. New experimental calibration in the system FeO-Al_2O_3-SiO_2-H_2O and certain P-T-X_{H2O} relations, Contrib. Mineral. Petrol. 116 (1994) 462–472.

[7] S. Sembiring, W. Simanjuntak, R. Situmeang, A. Riyanto, K. Sebayang, Preparation of refractory cordierite using amorphous rice husk silica for thermal insulation purposes, Ceram. Int. 42 (2016) 8431–8437.

[8] M.R. Boudchicha, F. Rubio, S. Achour, Synthesis of glass ceramics from kaolin and dolomite mixture, Int. J. Miner. Metall. Mater. 24 (2) (2017) 194–201.

[9] W. Wang, Z. Shin, X. Wang, W. Fan, The phase transformation and thermal expansion properties of cordierite ceramics prepared using drift sands to replace pure quartz, Ceram. Int. 42 (2016) 4477–4485.

[10] Y. Kobayashi, K. Sumi, E. Kato, Preparation of dense cordierite ceramics from magnesium compounds and kaolinite without additives, Ceram. Int. 26 (2000) 739–743.

[11] K. Sumi, Y. Kobayashi, E. Kato, Synthesis and sintering of cordierite from ultrafine particles of magnesium hydroxide and kaoline, J. Am. Ceram. Soc. 81 (4) (1998) 1029–1032.

[12] S.J. Lee, W.M. Kriven, Crystalisation and densification of nano-size amorphous cordierite powder prepared by a PVA solution-polymerisation route, J. Am. Ceram. Soc. 81 (10) (1998) 2605–2612.

[13] J.R. Oh, H. Imai, H. Hirashima, Effect of Al/Si ratio on crystallization of cordierite ceramics prepared by the sol-gel method, J. Ceram. Soc. Jpn. 105 (1) (1997) 43–47.

[14] M. Okuyama, T. Fukui, C. Sakurai, Effect of complex precursors on alkixide-derived cordierite powder, J. Am. Ceram. Soc. 75 (1) (1992) 153–160.

[15] Z.M. Shi, K.M. Liang, Q. Zhang, S.R. Gu, Effect of cerium addition on phase transformation and microstructure of cordierite ceramics prepared by sol-gel, J. Mater. Sci. 36 (2001) 5227–5230.

[16] G.T. Adylov, R.Y. Akbarov, S. Singh, M.A. Zufarov, G.V. Voronov, N.A. Kulagina, E.P. Mansurova, M.K. Rumi, Crystallisation of μ- and α-cordierite in glass obtained via melting by concentrated radiant flux, Appl. Sol. Energy 44 (2) (2008) 135–138.

[17] S.P. Hwang, J.M. Wu, Effect of composition on microstructural development in MgO-Al_2O_3-SiO_2 glass – ceramics, J. Am. Ceram. Soc. 84 (5) (2012) 1108–1112.

[18] K. Sumi, Y. Kobayashi, E. Kato, Low-temperature fabrication of cordierite ceramics from kaolinite and magnesium hydroxide mixtures with boron oxide additives, J. Am. Ceram. Soc. 82 (3) (1999) 783–785.

[19] R. Goren, H. Gocmez, C. Ozgur, Synthesis of cordierite powder from talc diatomite and alumina, Ceram. Int. 32 (2006) 407–409.

[20] B. Fotoohi, S. Blackburn, Study of phase transformation and microstructure in sintering of mechanically activated cordierite precursors, J. Am. Ceram. Soc. 95 (8) (2012) 2640–2646.

[21] S. Sembiring, W. Simanjuntak, R. Situmeang, A. Riyanto, P. Karo-Karo, Effect of alumina addition on the phase transformation and crystallisation properties of refractory cordierite prepared from amorphous rice husk silica, J. Asian Ceram. Soc. 5 (2) (2017) 186–192.

[22] D. Kuscer, I. Bantan, M. Hrovat, B. Malič, The microstructure, coefficient of thermal expansion and flexural strength of cordierite ceramics prepared from alumina with different particle sizes, J. Eur. Ceram. Soc. 37 (2) (2017) 739–746.

[23] A. Aşkin, I. Tatar, Ş. Kilinç, Ö. Tezel, The utilization of waste magnesite in the production of the cordierite ceramic, Energy Procedia 107 (2017) 137–143.

[24] A. Raghdi, M. Heraiz, F. Sahnoune, N. Saheb, Mullite-zirconia composites prepared from halloysite reaction sintered with boehmite and zirconia, Appl. Clay Sci. 146 (2017) 70–80.

[25] M.E. Miller, S.T. Misture, Stoiciometric (Ni, Mg)-cordierite glass-ceramics, J. Am. Ceram. Soc. 93 (2010) 1018–1024.

[26] S.M. Clark, The kinetic analysis of irreversible consecutive solid state reactions: the effect of zinc on the formation of cordierite, J. Am. Ceram. Soc. 100 (2017) 2525–2532.

[27] K. Watanabe, E.A. Giess, Crystallization kinetics of high-cordierite glass, J. Non Cryst. Sol. 169 (1994) 306–310.

[28] T. Rudolph, W. Pannhorst, G. Petzow, Determination of activation energies for the crystallization of a cordierite-type glass, J. Non Cryst. Sol. 155 (1993) 273–281.

[29] N.T. Silva, N.F. Nasciemento, L.S. Cividanes, C.A. Bertran, G.P. Thim, Kinetics of cordierite crystallisation from diphasic gels, J. Sol-Gel Sci. Technol. 47 (2008) 140–147.

[30] I.W. Donald, The crystallization kinetics of a glass based on the cordierite composition studied by DTA and DSC, J. Mater. Sci. 30 (1995) 904–915.

[31] D.B. Kim, K.H. Lee, Crystallization and sinterability of cordierite-based glass powders containing CeO2, J. Mater. Sci. 29 (1994) 6592–6598.

[32] A. Goel, E.R. Shaaban, M.J. Ribiero, F.C.L. Melo, J.M.F. Ferreira, Influence of NiO on the crystallization kinetics of near stoichiometric cordierite glasses nucleated with TiO_2, J. Phys. Condens. Matter 19 (2007) 386231.

[33] M.R. Boudchicha, F. Rubio, S. Achour, Synthesis of glass ceramics from kaolin and dolomite mixture, Int. J. Miner. Metall. Mater. 24 (2) (2017) 194–201.

[34] L. Song, J. Wu, Z. Li, X. Hao, Y. Yu, Crystallization mechanisms and properties of α-cordierite glass–ceramics from K2O–MgO–Al2O3–SiO2 glasses, J. Non-Cryst. Solids 419 (2015) 16–26.

[35] A. Goel, E.R. Shaaban, F.C.L. Melo, M.J. Ribeiro, J.M.F. Ferreira, Non-isothermal crystallization kinetic studies on MgO–Al2O3–SiO2–TiO2 glass, J. Non-Cryst. Solids 353 (2007) 2383–2391.

[36] Y. Hu, H.T. Tsai, The effect of BaO on the crystallization behaviour of a cordierite-type glass, Mater. Chem. Phys. 52 (1998) 18–C188.

[37] F. Sahnoune, M. Chegaar, N. Saheb, P. Goeuriot, F. Valdivieso, Algerian kaolinite used for mullite formation, Appl. Clay Sci. 38 (3) (2008) 304–310.

[38] F. Sahnoune, N. Saheb, B. Khamel, Z. Takkouk, Thermal analysis of dehydroxylation of Algerian kaolinite, J. Therm. Anal. Calorim. 107 (2012) 1067–1072.

[39] F. Sahnoune, M. Chegaar, N. Saheb, P. Goeuriot, F. Valdivieso, Differential thermal analysis of mullite formation from Algerian kaolin, Adv. Appl. Ceram. 107 (1) (2008) 9–13.

[40] A.W. Coats, J.P. Redfern, Kinetic parameters from thermogravimetric data, Nature 201 (1964) 68–69.
[41] J.A. Augis, J.E. Bennet, Calculation of Avrami parameters for heterogeneous solid-state reactions using a modification of Kissinger method, J. Therm. Anal. 13 (1978) 283–292.
[42] P.G. Boswell, On the calculation of activation energies using modified Kissinger method, J. Therm. Anal. 18 (1980) 353–358.
[43] T. Ozawa, A new method for analysing thermogravimetric data, Bull. Chem. Soc. Jpn. 38 (1965) 1881–1886.
[44] P. Ptáček, F. Šoukal, T. Opravil, J. Havlica, J. Brandštetr, Crystallization of spinel phase from metakaoline: the nonisothermalthermodilatometric CRH study, Powder Technol. 243 (2013) 40–45.
[45] M. Romero, J. Martı´n-Ma´rquez, J. Ma Rinco´n, Kinetic of mullite formation from a porcelain stoneware body for tiles production, J. Eur. Ceram. Soc. 26 (2006) 1647–1652.
[46] M.M.S. Sanad, M.M. Rashad, E.A. Abdel-Aal, K. Powers, Novel cordierite nano-powders of new crystallization aspects and its cordierite-based glass ceramics of improved mechanical and electrical properties for optimal use in multidisciplinary scopes, Mater. Chem. Phys. 162 (2015) 299–307.
[47] Chen Yung-Feng, M.C. Wang, M.H. Hon, Phase transformation and growth of mullite in kaolin ceramics, J. Eur. Ceram. Soc. 24 (2004) 2389–2397.
[48] O. Castelein, B. Soulestin, J.P. Bonnet, P. Blanchart, The influence of heating rate on the thermal behaviour and mullite formation from a kaolin raw material, Ceram. Int. 27 (2001) 517–522.
[49] M. Nikaido, Y. Yoshizawa, F. Saito, Effects of grinding on formation of mullite in a sintered body and its mechanical and thermal properties, J. Chem. Eng. Jpn. 29 (1996) 456–463.
[50] N.H.H. Phuc, T. Okuno, A. Matsuda, H. Muto, Ex situ Raman mapping study of mechanism of cordierite formation from stoichiometric oxide precursors, J. Eur. Ceram. Soc. 34 (2014) 1009–1015.
[51] C.Y. Chen, G.S. Lan, W.H. Tuan, Preparation of mullite by the reaction sintering of kaolinite and alumina, J. Eur. Ceram. Soc. 20 (2000) 2519–2525.
[52] A. Ş.ükran Demirkıran Tuğba Tunç, The effects of mechanical activation on the sintering and microstructural properties of cordierite produced from natural zeolite, Powder Technol. 260 (2014) 7–14.
[53] R. Bejjaoui, A. Benhammou, L. Nibou, B. Tanouti, J.P. Bonnet, A. Yaacoubi, A. Ammar, Synthesis and characterization of cordierite ceramic from Moroccan stevensite and andalusite, Appl. Clay Sci. 49 (2010) 336–340.
[54] B. Fotoohi, S. Blackburn, Effects of mechanochemical processing and doping of functional oxides on phase development in synthesis of cordierite, J. Eur. Ceram. Soc. 32 (2012) 2267–2272.
[55] J.B.R. Neto, R. Moreno, Effect of mechanical activation on the rheology and casting performance of kaolin/talc/alumina suspensions for manufacturing dense cordierite bodies, Appl. Clay Sci. 38 (2008) 209–218.
[56] W. Misra, M. Loutou, L. Saadi, M. Mansori, M. Waqif, C. Favotto, Cordierite containing ceramic membranes from smectetic clay using natural organic wastes as pore-forming agents, J. Asian Ceram. Soc. 5 (2) (2017) 199–208.